Stabilization of Type-I β-Turn Conformations in Peptides Containing the NPNA-Repeat Motif of the *Plasmodium falciparum* Circumsporozoite Protein by Substituting Proline for (*S*)-α-Methylproline

Christian Bisang,[†] Christoph Weber,[†] Janice Inglis,[†] Celia A. Schiffer,[‡,§] Wilfred F. van Gunsteren,[‡] Ilian Jelesarov,[∥] Hans R. Bosshard,[∥] and John A. Robinson*,[†]

Contribution from the Institutes of Organic Chemistry and Biochemistry, University of Zürich, 8057 Zürich, and Laboratory of Physical Chemistry, ETH-Zürich, 8092 Zürich, Switzerland

Received March 22, 1995[⊗]

Abstract: The immunologically dominant central portion of the circumsporozoite (CS) surface protein on the malaria parasite *Plasmodium falciparum* contains a large number of tandemly repeated NPNA tetrapeptide motifs. The preferred secondary structure of this repeat unit in aqueous solution has been investigated with the aid of the secondary structure-inducing amino acid (*S*)-α-methylproline (P^{Me}). ^{1}H-Nuclear magnetic resonance (NMR) and circular dichroism (CD) spectroscopy have been used to probe the structures of synthetic peptides containing one to three tetrapeptide $NP^{Me}NA$ units. The far-UV CD spectra of these peptides show more intense negative bands at 215 nm than do similar peptides based on the NPNA motif. This and the temperature dependence of the peptide amide chemical shifts, the pattern of NOE connectivities, and the magnitude of ^3J coupling constants, derived from one- and two-dimensional NMR spectra of $Ac(NP^{Me}NA)_3$-OH, provide strong evidence for stable turnlike structures. From NOE distance and dihedral angle restraints, structures consistent with the NMR parameters were calculated. These reveal a stable hydrogen-bonded type-I β-turn conformation (most likely present at 70−80% population) within each $NP^{Me}NA$ motif, stabilized by the backbone C_α methylation. Side chain to backbone hydrogen bonds involving the side chain amide groups of both asparagine residues also appear to impart stabilization to the turn conformation. No regular repeating conformations were detected in the linker regions connecting each $NP^{Me}NA$ unit. Polyclonal antisera raised in rabbits against $(NP^{Me}NA)_3$ recognized intact *P. falciparum* sporozoites in an immunofluorescence assay as efficiently as antisera raised against $(NPNA)_3$. This indicates that the type-I β-turn detected in the P^{Me}-containing peptide is closely related to the immunologically dominant portion of the folded CS protein. An improved knowledge of the three-dimensional structure of this protein may be of value for the design of second-generation synthetic malaria vaccines.

Introduction

The rapid growth in knowledge of the sequence and three-dimensional structure of proteins from pathogenic organisms has generated considerable interest in the design and development of synthetic peptide vaccines.[1,2] One of the problems to be overcome, however, is the difficulty of representing in a small molecule the conformational epitopes important for protective antibody production. Although neutralizing epitopes can sometimes be localized, for example, to loops or helixes on the surface of a protein, the corresponding regions as linear peptides will be more conformationally mobile and unlikely to adopt to the same extent a stable secondary structure in aqueous solution. For this reason linear peptide immunogens may sometimes fail to elicit antibodies capable of binding with high affinity to the cognate native protein antigen, or do so at low frequency.[3] This problem has been recognized for some time,[4] and attempts have been made already to induce a more efficient immune response by using conformationally restrained immunogens. Of course, a prerequisite is that the immunologically relevant conformer(s) is (are) known and that methods can be found to stabilize these selectively.

We describe here the use of a secondary structure-inducing non-proteinogenic amino acid, (*S*)-α-methylproline (P^{Me}), to study the immunologically important conformation of a synthetic peptide based on the tandemly repeated tetrapeptide Asn-Pro-Asn-Ala (NPNA), present in the major surface protein of the invasive sporozoite stage of *Plasmodium falciparum*,[5,6] the most virulent *Plasmodium* species known to cause malaria.[7,8] Recently, peptides containing this sequence were incorporated into the synthetic copolymer vaccine SPf66[9,10] and shown to induce partial protection against malaria in field trials in South

[†] Institute of Organic Chemistry, University of Zurich.
[‡] ETH-Zürich.
[§] Current address: Genentech Inc., 460 Point San Bruno Blvd., S. San Francisco, CA 94080-4990.
[∥] Institute of Biochemistry, University of Zurich.
* Address for correspondence: Prof. J. A. Robinson, Institute of Organic Chemistry, University of Zürich, Winterthurerstrasse 190, 8057 Zürich, Switzerland.
[⊗] Abstract published in *Advance ACS Abstracts*, July 1, 1995.

(1) Arnon, R.; Horwitz, R. J. *Curr. Opin. Immunol.* **1992**, *4*, 449.
(2) Brown, F. *Philos. Trans. R. Soc. London, Ser. B.* **1994**, *344*, 213.
(3) Van Regenmortel, M. H. V. *Trends Biochem. Sci.* **1987**, *12*, 237.
(4) (a) Schulze-Gahmen, U.; Klenk, H. D.; Beyreuther, K. *Eur. J. Biochem.* **1986**, *159*, 283. (b) Satterthwait, A. C.; Arrhenius, T.; Hagopian, R. A.; Zavala, F.; Nussenzweig, V.; Lerner, R. A. *Phil. Trans. R. Soc. London, Ser. B* **1989**, *323*, 565.
(5) Enea, V.; Ellis, J.; Zavala, F.; Arnot, D. E. *Science* **1984**, *225*, 628.
(6) Dame, J. B.; Williams, J. L.; McCutchan, T. F.; Weber, J. L.; Wirtz, R. A.; Hockmeyer, W. T.; Maloy, W. L.; Haynes, J. D.; Schneider, I.; Roberts, D.; Sanders, G. S.; Reddy, E. P.; Diggs, C. L.; Miler, L. H. *Science* **1984**, *225*, 593.
(7) Nussenzweig, R. S.; Long, C. A. *Science* **1994**, *265*, 1381.
(8) Miller, L. H.; Good, M. F.; Milon, G. *Science* **1994**, *264*, 1878.

0002-7863/95/1517-7904$09.00/0

America[11,12] and Africa.[13,14] These trials establish the feasibility of blood-stage vaccination in humans and provide a basis for attempts to improve its efficacy.

The immunologically dominant central portion of the *P. falciparum* circumsporozoite (CS) protein contains about 40 repeats of the NPNA tetrapeptide[5,6] and is presumed to adopt a more-or-less regular secondary structure. First generation sporozoite vaccines included NPNA repeats, either as synthetic peptide–protein conjugates[15] or as a recombinant protein.[16] Although no crystal structure of the CS protein is available, NMR and CD studies[17,18] of peptides containing tandemly repeated NANP or NPNA tetrapeptide motifs indicated the presence of conformers containing helical and/or reverse turns based on the NPNA cadence,[18] in rapid dynamic equilibrium with unfolded forms.

Our interest in this problem stems from earlier observations[19] showing that, when proline is present at position $i + 1$ in a tetrapeptide sequence with a high intrinsic propensity to adopt turn conformations, the replacement of this proline by P^{Me} can lead to a significant stabilization of β-turn conformations in the dynamic equilibrium with unfolded forms. Moreover, it was shown that this substitution in a peptide antigen can result in an improved affinity to complementary anti-peptide monoclonal antibodies.[19] In this paper, we report the synthesis of peptides containing the $NP^{Me}NA$ tetrapeptide, as a single unit and tandemly repeated [i.e., $(NP^{Me}NA)_n$; $n = 1, 2$, or 3], the results of ^{1}H-NMR and CD studies of their conformational behavior, and the properties of polyclonal antisera raised in rabbits against the trimer conjugated to keyhole limpet hemocyanin. Through replacement of proline by P^{Me} we observe in aqueous solution a significant stabilization of secondary structure within the NP^{Me}-NA motif, in particular a type-I β-turn with a dynamic interconversion between forms with the side chains of Asn (i) and Asn ($i + 2$) hydrogen bonded to the peptide backbone. The biological relevance of these folded forms in the native sequence is indicated by the ability of the above-mentioned polyclonal anti-$(NP^{Me}NA)_3$ antisera to strongly bind *P. falciparum* sporozoites in a solid-phase immunofluorescence assay.

Scheme 1

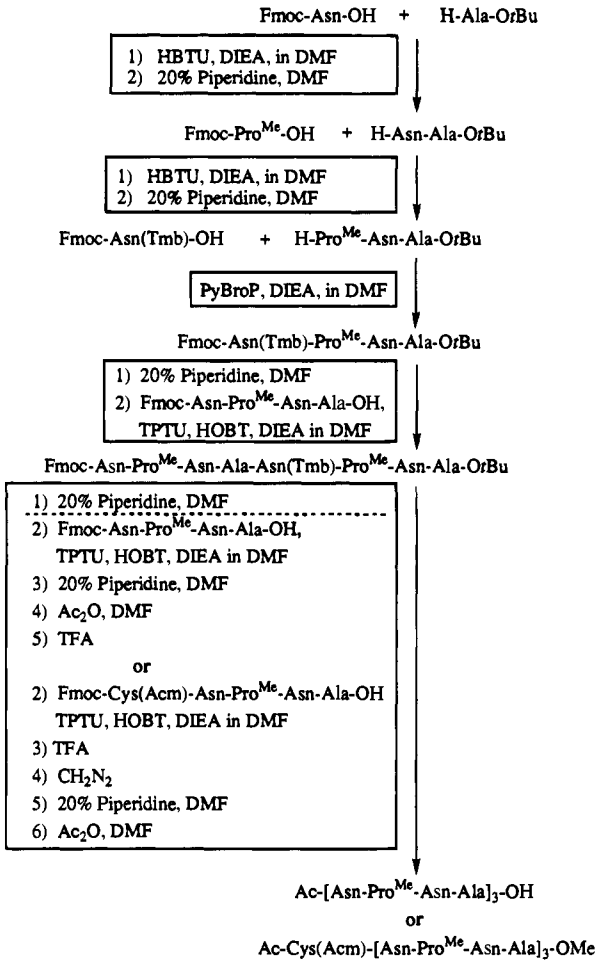

Results

Synthesis. Whereas the synthesis of the peptide Ac-$(NPNA)_3$-OH could be carried out using standard solid-phase peptide synthetic methods, with the Fmoc chemistry,[20] attempts to construct the methylated peptide Ac-$(NP^{Me}NA)_3$-OH in the same way gave a complex mixture of peptides, due to difficulties in coupling efficiently onto P^{Me}. Steric hindrance slowed the acylation of P^{Me} on the solid phase, as well as in free solution, using HBTU[21,22] or PyBroP[23] activation, and was incomplete even with prolonged coupling times. For this reason the P^{Me}-containing peptides used for later studies were prepared in solution by the route shown in Scheme 1. The corresponding C-terminal methyl esters were prepared by treatment of the free acids with diazomethane.

Toward the end of this work, the use of HATU in solid-phase peptide synthesis was reported.[24] Such 7-azabenzotriazole-based coupling reagents give activated amino acids showing enhanced reactivity and appear to be especially suited for the preparation of peptides containing hindered amino acids. The solid-phase synthesis of Ac-$(NP^{Me}NA)_3$-OH was therefore repeated, using the Fmoc chemistry and HATU for activation.

(9) Patarroyo, M. E.; Amador, R.; Clavijo, P.; Moreno, A.; Guzman, F.; Romero, P.; Tascon, R.; Franco, A.; Murillo, L. A.; Ponton, G.; Trujillo, G. *Nature* **1988**, *332*, 158.

(10) Patarroyo, M. E.; Romero, P.; Torres, M. L.; Clavijo, P.; Moreno, A.; Martínez, A.; Rodríguez, R.; Guzman, F.; Cabezas, E. *Nature* **1987**, *328*, 629.

(11) Sempértegui, F.; Estrella, B.; Moscoso, J.; Piedrahita C. L.; Hernández, D.; Gaybor, J.; Naranjo, P.; Mancero, O.; Arias, S.; Bernal, R.; Córdova, M. E.; Suárez, J.; Zicker, F. *Vaccine* **1994**, *12*, 337.

(12) Valero, M. V.; Amador, L. R.; Galindo, C.; Figueroa, J.; Bello, M. S.; Murillo, L. A.; Mora, A. L.; Patarroyo, G.; Rocha, C. L.; Rojas, M.; Aponte, J. J.; Sarmiento, L. E.; Lozada, D. M.; Coronell, C. G.; Ortega, N. M.; Rosas, J. E.; Alonso, P. L.; Patarroyo, M. E. *Lancet* **1993**, *341*, 705.

(13) Alonso, P. L.; Tanner, M.; Smith, T.; Hayes, R. J.; Armstrong Schellenberg, J.; Lopez, M. C.; Bastos de Azevedo, I.; Menendez, C.; Lyimo, E.; Weiss, N.; Kilama, W. L.; Teuscher, T. *Vaccine* **1994**, *12*, 181.

(14) Teuscher, T.; Armstrong Schellenberg, J. R. M.; Bastos de Azevedo, I.; Hurt, N.; Smith, T.; Hayes, R.; Masanja, H.; Silva, Y.; Lopez, M. C.; Kitua, A.; Kilama, W.; Tanner, M.; Alonson, P. L. *Vaccine* **1994**, *12*, 328.

(15) (a) Herrington, D. A.; Clyde, D. F.; Losonsky, G.; Cortesia, M.; Murphy, J. R.; Davis, J.; Baqar, S.; Felix, A. M.; Heimer, E. P.; Gillessen, D.; Nardin, E.; Nussenzweig, R. S.; Nussenzweig, V.; Hollingdale, M. R.; Levine, M. M. *Nature* **1987**, *328*, 257. (b) Etlinger, H. M.; Felix, A. M.; Gillessen, D.; Heimer, E. P.; Just, M.; Pink, J. R. L.; Sinigaglia, F.; Sturchler, D.; Takacs, B.; Trzeciak, A.; Matile, H. *J. Immunol.* **1988**, *140*, 626.

(16) Ballou, W. R.; Sherwood, J. A.; Neva, F. A.; Gordon, D. M.; Wirtz, R. A.; Wasserman, G. F.; Diggs, C. L.; Hoffman, S. L.; Hollingdale, M. R.; Hockmeyer, W. T.; Schneider, I.; Young, J. F.; Reeve, P.; Chulay, J. D. *Lancet* **1987**, 1277.

(17) Esposito, G.; Pessi, A.; Verdini, A. S. *Biopolymers* **1989**, *28*, 225.

(18) Dyson, H. J.; Satterthwait, A. C.; Lerner, R. A.; Wright, P. E. *Biochemistry* **1990**, *29*, 7828.

(19) Hinds, M.; Welsh, J. H.; Brennand, D. M.; Fisher, J.; Glennie, M. J.; Richards, N. G. J.; Turner, D. L.; Robinson, J. A. *J. Med. Chem.* **1991**, *34*, 1777.

(20) Atherton, E.; Sheppard, R. C. *Solid phase peptide synthesis—a practical approach*; IRL Press: Oxford, U.K., 1989.

(21) Dourtoglou, V.; Gross, B.; Lamropoulou, V.; Zioudrou, C. *Synthesis* **1984**, 572.

(22) Knorr, R.; Trzeciak, A.; Bannwarth, W.; Gillessen, D. *Tetrahedron Lett.* **1989**, *30*, 1927.

(23) Frérot, E.; Coste, J.; Pantaloni, A.; Marie-Noëlle, D.; Jouin, P. *Tetrahedron* **1991**, *47*, 259.

(24) (a) Carpino, L. A. *J. Am. Chem. Soc.* **1993**, *115*, 4397. (b) Carpino, L.; El-Faham, A.; Minor, C. A.; Albericio, F. *J. Chem. Soc., Chem. Commun.* **1994**, 201.

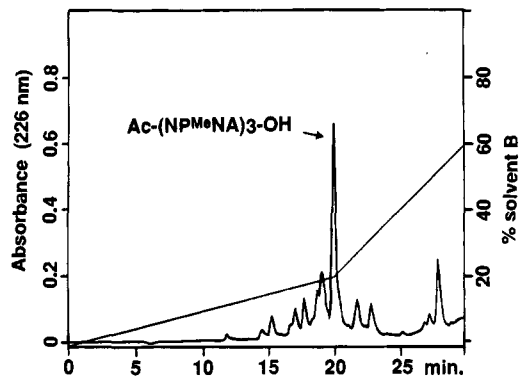

Figure 1. HPLC chromatogram of products from the solid-phase synthesis of Ac-(NP^{Me}NA)$_3$-OH using HATU activation,[24] on a Waters μ-Bondapak C_{18} 25 × 100 mm preparative HPLC cartridge with a gradient of 0−20% acetonitrile in water over 20 min with 0.1% TFA. Detection was by UV adsorption at 226 nm. The peak corresponding to Ac-(NP^{Me}NA)$_3$-OH is indicated.

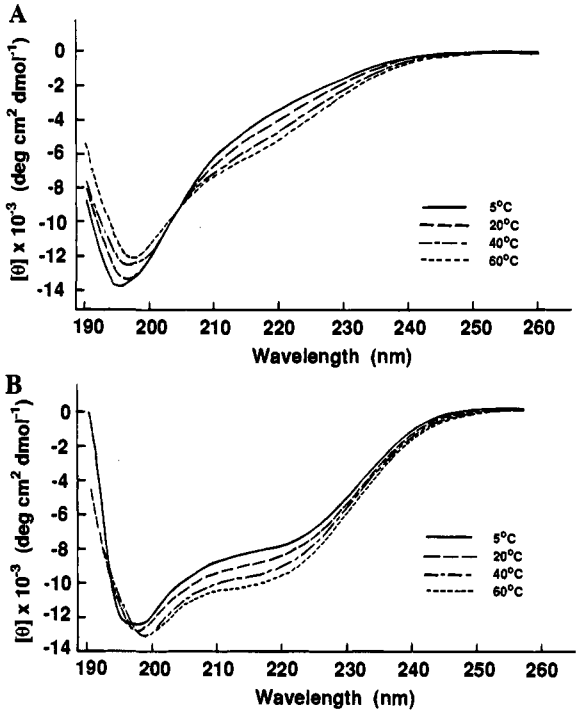

Figure 2. Far-UV CD spectrum of (A) Ac-(NPNA)$_3$-OH and (B), Ac-(NP^{Me}NA)$_3$-OH at 5, 20, 40, and 60 °C in 5 mM phosphate buffer, pH 5.0 (see the Experimental Section).

The first seven residues were incorporated in high yield using single coupling cycles, each with 3 equiv of activated amino acid. The acylation of subsequent P^{Me} residues on the solid phase, however, required three or four coupling cycles, each with 3 equiv of Fmoc-Asn(Mtt)-OH. Residual free amino groups were then capped with benzoic anhydride. Upon completion of the synthesis and cleavage of the peptide from the resin with TFA, the major product was the desired 12-mer peptide, which could be easily purified by reverse-phase HPLC (Figure 1) in 26% (unoptimized) yield. This successful use of HATU simplifies considerably the preparation of these P^{Me}-containing peptides and augers well for the rapid solid-phase assembly of other NPNA derivatives modified by backbone methylation, as well as the wider application of α-methylproline in peptide structure−function studies.

CD Spectra. The far-UV CD spectra of Ac-(NPNA)$_3$-OH (Figure 2A) and Ac-(NPNA)$_3$-OMe (data not shown), in 5 mM phosphate buffer, pH 5.0, are essentially identical, with negative maxima at ≈195 nm. As the temperature is raised from 5 to 60 °C the negative maximum at 195 nm decreases slightly in intensity and moves to 198 nm, whereas the negative ellipticity at 218 nm increases in intensity and becomes a distinct shoulder. In contrast, the CD spectra of Ac-(NP^{Me}NA)$_3$-OH (Figure 2B) and Ac-(NP^{Me}NA)$_3$-OMe (data not shown) show a negative cotton effect at ≈198 nm as well as a far more pronounced negative ellipticity near 215 nm, indicative of a more ordered conformation in the P^{Me}-containing peptide. Moreover, this negative ellipticity at 215 nm again increases in intensity with temperature. It is well-known that peptides having α-helical secondary structure show CD spectra with a minimum at 222 nm (helical $n \rightarrow \pi^*$ transition) and a second minimum between 200 and 208 nm (overlapping helical and random coil $\pi \rightarrow \pi^*$ transitions). In many cases the negative peak at 222 nm decreases in intensity with increasing temperature, due to thermal unfolding of the α-helix (see for example ref 25). An increase in negative CD amplitude at 222 nm with temperature is less common but has been seen,[26] for example, with largely unstructured peptides that do not show a genuine negative CD maximum at 222 nm. However, the temperature-dependent far-UV CD properties of a 60-residue proline-rich neutralization domain from feline leukemia virus[27] are very similar in shape to those shown in Figure 2B. The significant increase in negative ellipticity at ≈215 nm seen with Ac-(NP^{Me}NA)$_3$-OH may reflect an increased population of structured forms at higher temperatures, including turn conformations (vide infra). One can speculate that if the unstructured peptide interacts with more solvent molecules (e.g., through hydrogen bonding) than do(es) the structured form(s), then the principal driving force for folding would be the increased entropy of the system (i.e., an endothermic reaction) resulting from the release of water molecules to the bulk solvent.[28]

NMR. The 1D ^{1}H-NMR spectrum of the peptide Ac-(NPNA)$_3$-OH shows the presence of a minor component (<10%), due to *cis*−*trans* isomerism about one or more of the Asn-Pro peptide bonds, as observed in previous studies.[18] The appearance of resonances from only a single species (i.e., >99% homogeneous) in the ^{1}H-NMR spectrum of Ac-(NP^{Me}NA)$_3$-OH is consistent with this, since the *cis* rotamer is more strongly disfavored at Asn-P^{Me} peptide bonds. More importantly, the problems of resonance overlap caused by the tandem duplication of the proton environments in the repeating units are less severe in the methylated peptide; the peptide NH resonances in the spectrum of Ac(NP^{Me}NA)$_3$-OH as well as the C_βH resonances from each of the Asn residues can now be resolved, and the improved spectral dispersion allows measurement of individual Asn $^3J_{\alpha\beta}$ coupling constants from resolution enhanced one-dimensional spectra (with reference to COSY spectra for determination of peak positions and multiplet appearance).

The NMR assignments given in Table 1 were achieved straightforwardly using standard methods[29] at 600 MHz. Individual spin system assignments were obtained using TOCSY and DQF-COSY spectra, and analysis of NOESY spectra afforded sequential assignments. The α-methyl resonances of

(25) Shoemaker, K. R.; Kim, P. S.; York, E. J.; Stewart, J. M.; Baldwin, R. L. *Nature* **1987**, *326*, 563.
(26) (a) Shoemaker, K. R.; Fairman, R.; York, E. J.; Stewart, J. M.; Baldwin, R. L. In *Petides—Chemistry and Biology*; Proceedings of the 10th American Peptide Symposium; Marshall, G. R., Ed.; ESCOM: Leiden, The Netherlands, 1988; pp 15−20. (b) Forood, B.; Feliciano, E. J.; Nambiar, K. P. *Proc. Natl. Acad. Sci. U.S.A.* **1993**, *90*, 838 (c) Jasanoff, A.; Fersht, A. R. *Biochemistry* **1994**, *33*, 2129. (d) Ilyina, E.; Milius, R.; Mayo, K. H. *Biochemistry* **1994**, *33*, 13436.
(27) Fontenot, J. D.; Tjandra, N.; Ho, C.; Andrews, P. C.; Montelaro, R. C. *J. Biomol. Struct. Dyn.* **1994**, *11*, 821.
(28) Doty, P.; Yang, J. T. *J. Am. Chem. Soc.* **1956**, *78*, 498.
(29) Wüthrich, K. *NMR of Proteins and Nucleic Acids*; J. Wiley & Sons: New York, 1986.

Table 1. Chemical Shift Assignments for Peptides at 278 K

residue	chemical shift (ppm)[a] NH	$C^{\alpha}H$	$C^{\beta}H/C^{\gamma}H$	others
		Ac-NP^{Me}NA-OH		
Asn 1	8.54	4.91	*2.75, 2.90*[c]	NH^Z 7.17, NH^E 7.86
P^{Me} 2[b]		1.53	1.97−2.12[d]	$C^{\delta}H_2$ 3.91, 4.02
Asn 3	8.11	4.82	2.64, 2.97	NH^Z 7.08, NH^E 7.80
Ala 4	7.62	4.03	1.41	
		Ac-(NP^{Me}NA)$_2$-OH		
Asn 1	8.55	4.90	*2.74, 2.89*[c]	NH^Z 7.17, NH^E 7.85
P^{Me} 2[b]		1.52	1.97−2.16[d]	$C^{\delta}H_2$ 3.91, 4.02
Asn 3	8.15	4.72	2.68, 2.91	NH^Z 7.09, NH^E 7.77
Ala 4	7.81	4.20	1.43	
Asn 5	8.52	4.96	*2.78, 2.96*[c]	NH^Z 7.17, NH^E 7.84
P^{Me} 6[b]		1.53	1.97−2.16[d]	$C^{\delta}H_2$ 3.91, 3.97
Asn 7	8.09	4.83	2.64, 2.98	NH^Z 7.10, NH^E 7.80
Ala 8	7.59	4.04	1.42	
		Ac-(NP^{Me}NA)$_3$-OH		
Asn 1	8.55	4.89	*2.74, 2.89*[c]	NH^Z 7.16, NH^E 7.85
P^{Me} 2[b]		1.52	1.95−2.14[d]	$C^{\delta}H_2$ 3.89, 4.01
Asn 3	8.16	4.69	2.68, 2.90	NH^Z 7.08, NH^E 7.77
Ala 4	7.82	4.20	1.43	
Asn 5	8.45	4.94	*2.77, 2.95*[c]	NH^Z 7.16, NH^E 7.83
P^{Me} 6[b]		1.51	1.95−2.14[d]	$C^{\delta}H_2$ 3.85−3.95
Asn 7	8.14	4.72	2.67, 2.92	NH^Z 7.09, NH^E 7.78
Ala 8	7.79	4.20	1.43	
Asn 9	8.53	4.94	*2.79, 2.96*[c]	NH^Z 7.16, NH^E 7.84
P^{Me} 10[b]		1.53	1.95−2.14[d]	$C^{\delta}H_2$ 3.89, 3.96
Asn 11	8.09	4.83	2.63, 2.98	NH^Z 7.09, NH^E 7.81
Ala 12	7.58	4.03	1.42	

[a] Chemical shifts for $C_{\alpha}H$ protons are taken from DQF-COSY spectra. Those for the $C^{\delta}H_2$ protons of P^{Me} and the *E* and *Z* asparagine side chain amide protons are taken from ROESY spectra (τ_m = 300 ms). All other chemical shifts were determined in 1D spectra. [b] The assignment of the α-methyl group of P^{Me} is given in place of the $C^{\alpha}H$. [c] Stereospecific assignments at prochiral methylene groups are given in italics in the order pro-*S*/pro-*R*. [d] Indicates $C^{\beta}H_2$ and $C^{\gamma}H_2$ resonances of P^{Me} that are overlapped.

prolines were assigned on the basis of intra-residue and sequential NOEs, including $d_{\alpha N}$ NOEs between each P^{Me} and the following Asn. Asparagine side chain amide resonances were assigned on the basis of the characteristic NOE from the *E*-amide NH proton to the Asn $C_{\beta}H$'s and the strong correlation peak between the *E*- and *Z*-amide protons in a COSY spectrum. Neither the chemical shifts nor the line widths change significantly between 0.1 and 16 mM peptide concentration, indicating that aggregation does not occur under the conditions used.

Inspection of NOEs from NOESY spectra, in addition to amide proton temperature coefficients, and $^3J_{HN\alpha}$ and $^3J_{\alpha\beta}$ coupling constants, provides information on the types of conformers populated in aqueous solution. Since qualitatively and quantitatively comparable data concerning the preferred conformations within a single NP^{Me}NA repeat were obtained with Ac-NP^{Me}NA-OH, Ac-(NP^{Me}NA)$_2$-OH, and Ac-(NP^{Me}NA)$_3$-OH, as well as with the corresponding C-terminal methyl esters, and Ac-C(Acm)-(NP^{Me}NA)$_3$-OH and Ac-C(Acm)-(NP^{Me}NA)$_3$-OMe, only the results pertaining to Ac-(NP^{Me}NA)$_3$-OH will be described here in detail.

The temperature coefficients for the peptide amide NH resonances of Ac-(NP^{Me}NA)$_3$-OH, measured over the range 276−318 K, are shown in Table 2. For comparison, the corresponding values for Ac-(NPNA)$_3$-NH_2, determined by Dyson and co-workers, are also presented.[18] The $^3J_{HN\alpha}$ and $^3J_{\alpha\beta}$ coupling constants could be extracted directly from the 1D spectrum of Ac-(NP^{Me}NA)$_3$-OH, and these are also shown in Table 2. A pronounced periodicity in the temperature coefficients and the coupling constants is apparent between successive NP^{Me}NA motifs in the peptide Ac-(NP^{Me}NA)$_3$-OH. The

Table 2. Coupling Constants (Hz) and Temperature Coefficients × 10^3, ppm/K) for Peptide Amide NH Resonances

residue	$^3J_{\alpha N}$[a]	$^3J_{\alpha\beta}$[a]	$-\Delta\delta/\Delta T$[b]
	Ac-NP^{Me}NA-OH		
Asn 1	6.8	*5.6, 9.6*[c]	10.3
Asn 3	8.8	11.0, 4.0	5.6
Ala 4	6.0	7.3	2.6
	Ac-(NP^{Me}NA)$_2$-OH		
Asn 1	6.9	*5.6, 9.5*[c]	8.4
Asn 3	8.0	10.2, 4.6	5.4
Ala 4	5.9	7.2	2.0
Asn 5	7.5	*5.6, 9.8*[c]	8.5
Asn 7	8.7	10.6, 4.5	4.4
Ala 8	6.3	7.3	1.5
	Ac-(NP^{Me}NA)$_3$-OH		
Asn 1	6.9	*5.4, 10.1*[c]	8.4
Asn 3	8.0	10.3, 4.7	5.4
Ala 4	5.8	7.3	2.1
Asn 5	7.4	*5.7, 9.8*[c]	8.5
Asn 7	8.0	10.7, 4.5	5.4
Ala 8	5.6	7.3	1.5
Asn 9	7.4	*5.3, 10.6*[c]	9.0
Asn 11	8.8	11.2, 4.2	4.5
Ala 12	5.9	7.4	1.5
	Ac-(NPNA)$_3$-NH_2		
Asn 1	7.0		8.12
Asn 3	7.5		6.11
Ala 4	5.9		6.04
Asn 5	7.5		7.93
Asn 7	7.5		5.96
Ala 8	5.9		5.67
Asn 9	7.5		7.93
Asn 11	7.5		6.09
Ala 12	5.9		5.93

[a] Coupling constants were taken from 1D spectra (600 MHz) at 278 K (see text). Data for Ac-(NPNA)$_3$-NH_2 are from Dyson et al.[18] [b] Temperature coefficients for Ac-(NP^{Me}NA)$_n$-OH (n = 1, 2, 3) were calculated using at least 10 chemical shifts for each NH-proton, determined from 300 MHz 1D spectra recorded between 276 and 318 K. Those for Ac-(NPNA)$_3$-NH_2 were reported by Dyson et al.[18] [c] Stereospecific assignments at prochiral methylene groups are given in italics in the order pro-*S*/pro-*R*.

Ala-4, Ala-8, and Ala-12 peptide NH resonances, in particular, have significantly lower temperature coefficients than those for the other residues, indicative of the selective shielding of these groups from the bulk solvent. The Asn-3, -7, and -11 peptide NH temperature coefficients are also significantly smaller than the value expected (≈−7 to −9 ppb/K) for a fully solvent-exposed peptide amide proton. Furthermore, the $^3J_{\alpha\beta}$ coupling constants for this peptide are indicative of similar preferred side chain conformations for the Asn residues at equivalent positions within each NP^{Me}NA motif.

For the analysis of NOE connectivities a series of ROESY and NOESY spectra were measured, each with 100, 200, and 300 ms mixing times, for both Ac-(NP^{Me}NA)$_3$-OH and Ac-(NPNA)$_3$-OH. Having both ROESY and NOESY data available provided a check on the consistency of the NOEs observed and facilitated the calculation of average solution structures, as detailed below. For each peptide essentially the same NOE connectivities were apparent in both the ROESY and NOESY spectra, and the NOE connectivities derived for Ac-(NPNA)$_3$-OH were the same as those observed in previous studies[18] with Ac-(NPNA)$_3$-NH_2. Going from a free carboxylic acid at the C terminus to a methyl ester or an amide does not have a significant influence on the appearance of NOE cross peaks and so does not alter the preferred conformations of otherwise identical peptides under the conditions used.

The observed NOE connectivities are summarized in Figure 3. Portions of the ROESY spectrum of peptide Ac-(NP^{Me}NA)$_3$-

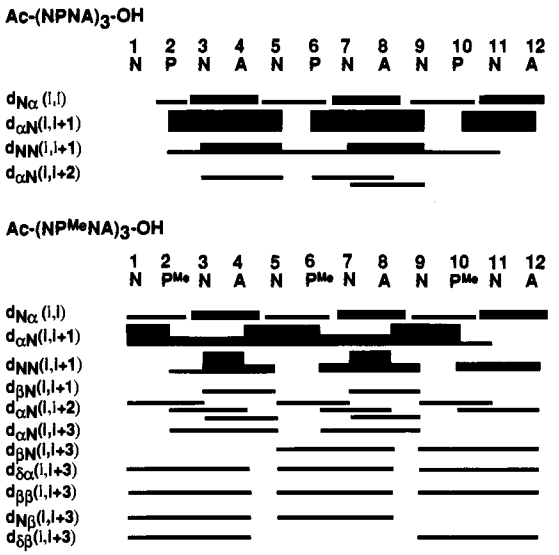

Figure 3. Summary of NOE connectivities observed for Ac-(NPNA)$_3$-OH and Ac-(NP^{Me}NA)$_3$-OH at 278 K. Data are from NOESY and ROESY spectra with a mixing time (spin-lock period) of 300 ms. NOE connectivities with Pro or P^{Me} are to C$_\delta$H's in place of NH.

OH are shown in Figure 4. A pronounced periodicity of NOE intensities is apparent between successive NP^{Me}NA motifs, which is also seen in the unmethylated peptide, albeit to a lesser degree. For both Ac-(NP^{Me}NA)$_3$-OH and Ac-(NPNA)$_3$-OH there are $d_{N\alpha}$ and $d_{\alpha N}(i, i + 1)$ NOE connectivities of differing intensities throughout the peptide backbone (Figure 4A), including connectivities to the proline C$^\delta$H protons, which may be used in place of the NH for proline.[30] Although both peptides show $d_{NN}(i, i + 1)$ NOE connectivities, the NOEs between the peptide NHs of adjacent Asn $(i + 2)$-Ala $(i + 3)$ residues in each tetrapeptide motif of the methylated peptide are particularly strong (Figure 4B). This is consistent with these residues lying at positions $i + 2$ and $i + 3$ of a β-turn, which would bring these peptide NHs into close proximity.[31] Numerous medium-range NOE connectivities are also apparent in the P^{Me}-containing peptide, that are either absent or weak and difficult to assign due to spectral overlap in the spectra of Ac-(NPNA)$_3$-OH. These include not only $d_{\alpha N}(i, i + 2)$ but also $d_{\alpha N}(i, i + 3)$ backbone connectivities and several $(i, i + 3)$ side chain−backbone and side chain−side chain connectivities (Figure 3), which may be taken as indicators of turn formation.[32] As an example, Figure 5A shows $d_{\beta\beta}(i, i + 3)$ NOE connectivities between Asn and Ala side chains in the peptide Ac-(NP^{Me}NA)$_3$-OH. The spectral dispersion is sufficient to allow unambiguous assignments of these NOEs. In the peptide Ac-(NPNA)$_3$-OH, on the other hand, a single weak Asn (i)−Ala $(i + 3)$ C$^\beta$H cross peak is seen at the resonance position of the badly overlapping Asn C$^\beta$H and Ala methyl groups (Figure 5B). Taken together, the temperature coefficients of the amide proton chemical shifts, the measured coupling constants, and the NOE connectivities, in particular between Asn (i) and Ala $(i + 3)$ residues within each NP^{Me}NA tetrapeptide motif, provide strong evidence for the occurrence of turn conformations in the methylated peptide that are significantly more stable than those in the peptide Ac-(NPNA)$_3$-OH. This prompted an attempt to determine average solution conformations for the NP^{Me}NA motif. Hence, cross peak volumes in the NOESY spectra of Ac-(NP^{Me}NA)$_3$-OH at 278 K with mixing times of 100, 200, and 300 ms were

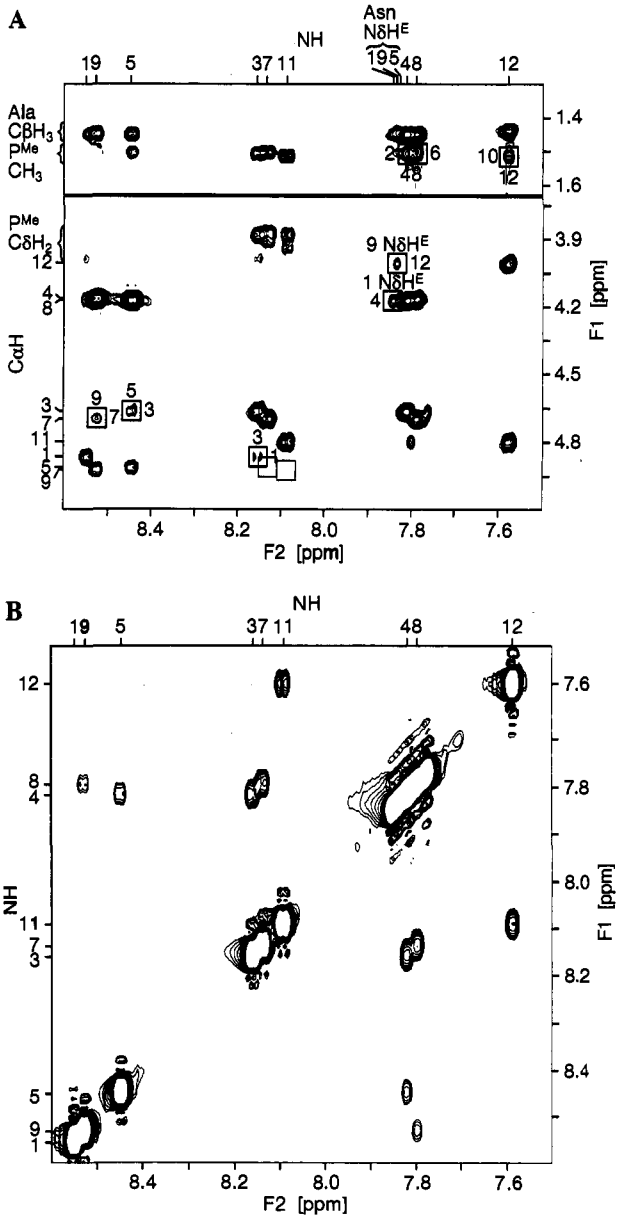

Figure 4. Portions of the ROESY spectrum (300 ms spin-lock time) of Ac-(NP^{Me}NA)$_3$-OH showing (A) the NH to C$_\alpha$H/C$_\beta$H connectivities and (B) the NH to NH connectivities. The numbers on the axes are the residue numbers for assignments and the chemical shifts in ppm. Some medium-range connectivities are highlighted in boxes.

determined using the FELIX software (see the Experimental Section). These cross peak volumes were converted into distances by referencing against a $d_{\alpha N}$ distance for Ala-4 and Asn-5 as well as Ala-8 and Asn-9 of 2.2 Å, the shortest sterically possible distance, and assuming an r^{-6} dependence of the NOE intensity on distance (r). To take account of possible spin diffusion effects, the NOE intensity-to-distance conversion was performed in three different ways (see the Experimental Section). The $d_{\alpha\beta}$ distances derived from the NOE build-up curves were found to be unusually long (3.0−3.5 Å) due to nonvanishing contributions from through-bond couplings, so analogous ROE build-up curves were used for $d_{\alpha\beta}$ distance estimations. For structure calculations, the estimated distances were grouped into three classes; those below 2.5 Å were assigned an upper limit of 2.7 Å, those below 3.0 Å an upper limit of 3.2 Å, and the remainder an upper limit of 5.0 Å. All distances involving residues more than one sequence position apart were also assigned an upper limit of 5 Å. This conservative classification was deemed necessary to allow for uncertain-

(30) Wüthrich, K.; Billeter, M.; Braun, W. *J. Mol. Biol.* **1984**, *180*, 715.
(31) Wright, P. E.; Dyson, H. J.; Lerner, R. A. *Biochemistry* **1988**, *27*, 7167.
(32) Dyson, H. J.; Wright, P. E. *Annu. Rev. Biophys. Biophys. Chem.* **1991**, *20*, 519.

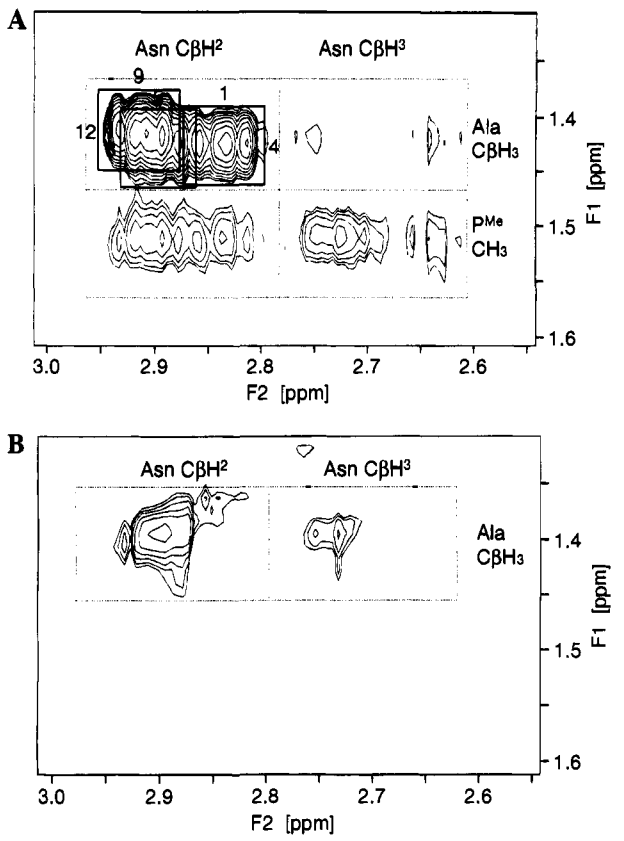

Figure 5. (A) Portion of a NOESY spectrum (300 ms mixing time) of Ac-(NP^{Me}NA)$_3$-OH showing $d_{\beta\beta}(i, i+3)$ NOE connectivities. (B) Corresponding region from a NOESY spectrum of Ac-(NPNA)$_3$-OH.

ties about possible nonlinear motional averaging and other multispin effects,[29] which have been ignored here in using the r^{-6} dependency of NOE intensity on distance, as well as for residual errors in the cross peak integration and distance calculations.

Local distance constraints derived from NOE measurements and $^3J_{HN\alpha}$ and $^3J_{\alpha\beta}$ coupling constants were also used as input for the program HABAS.[33] Using default program settings, an unambiguous stereospecific assignment of the Asn (i) C$^\beta$H's was possible, and the calculations yielded constraints for nine ϕ angles, six ψ angles, and six χ_1 angles. A full list of the distance and angle constraints used for the calculations is presented in the supplementary information.

Structure Calculations. Using 67 upper distance constraints, 3 lower distance constraints, and 21 angle constraints as input for the distance geometry program DIANA,[34] it was possible to calculate average solution conformations for the peptide Ac-(NP^{Me}NA)$_3$-OH. The first 25 structures with a final target function value below 0.1 Å^2 were then accepted for restrained molecular dynamics (MD) refinement, using the program GROMOS.[35] Thereafter, conformations of the peptide were eliminated if any of the remaining distance restraint violations were greater than 0.35 Å. On this basis 17 structures were selected for analysis.

Structure Analysis. All 17 refined structures of Ac-(NP^{Me}NA)$_3$-OH from the MD calculations contain a sequence of three consecutive type-I β-turns, one within each NP^{Me}NA repeat unit (Figures 6 and 7), but connected by largely irregular (i.e., conformationally mobile) hinges at the A−N junctions between these motifs. The rms deviations for all backbone atoms in each turn motif lie in the range 0.41−0.56 Å (see Table 3), indicating a high level of convergence between the turns in all 17 structures, as evidenced also by the superimpositions shown in Figure 6. Since the linker region between the individual motifs appears to be quite flexible, a superposition of the entire peptide chain from all 17 structures is not informative. The observed ϕ and ψ angles (Table 4) for P^{Me} ($i+1$) and Asn ($i+2$) residues within each turn motif approximate closely the dihedral angles for a "perfect" type-I β-turn.[36]

A search for hydrogen bonds using the default criteria in INSIGHT II (BIOSYM, Inc., San Diego, CA) revealed that the NH of Ala ($i+3$) and backbone CO of Asn (i) point toward each other, and lie within hydrogen-bonding distance, in almost all NP^{Me}NA motifs in the 17 structures (Figure 6D). There is an additional hydrogen-bonding possibility between the side chain O$^\gamma$ atom of Asn (i) and the backbone NH of Asn ($i+2$), although its geometry is in many cases less than ideal. A further hydrogen bond may arise between the O$^\gamma$ atom of Asn ($i+2$) and its own backbone NH group. These features can also be readily seen in Figure 7. The involvement of the Asn ($i+2$) and Ala ($i+3$) backbone NH's in intramolecular hydrogen bonds at the observed frequencies is consistent with the relatively low NH chemical shift temperature coefficients seen for these amide protons (see Table 2). The relatively few distance constraints between groups in adjacent NP^{Me}NA turn motifs reflect the paucity of such medium-range NOE connectivities in NOESY and ROESY spectra and point to a greater conformational mobility, in particular around the ψ angle of Ala ($i+3$) and ϕ of Asn (i).

No clear conclusions concerning the conformational dynamics of the P^{Me} residues can be drawn form the NMR data described above. In peptides and proteins containing proline, both the C$^\gamma$-exo (or UP) and C$^\gamma$-endo (or DOWN) puckered conformations of the pyrrolidine ring have been observed[37] and may interconvert rapidly. In our work, the lack of a $^3J_{\alpha\beta}$ coupling constant in P^{Me} removes one convenient assay for rapid conformational averaging between these different puckered forms.[38] Also, it is not yet clear to what extent the α-methyl group influences the preferred puckered conformations of the pyrrolidine ring. However, the P^{Me} residues within the final 17 MD refined structures adopt largely the C$^\gamma$-endo conformation, although C$^\gamma$-exo and other twist forms are also present.

Biological Activity. Polyclonal rabbit antisera were raised against the peptides Ac-C(NPNA)$_3$-OMe and Ac-C(NP^{Me}NA)$_3$-OMe, each conjugated through the cysteine residue to keyhole limpet hemocyanin (KLH). The IgG fraction from each antiserum was isolated by protein-A affinity chromatography and tested by ELISA for binding to Ac-C(NPNA)$_3$-OMe conjugated to bovine serum albumin (BSA). Both antisera showed a comparably high titer of cross-reactive antibodies (Figure 8). A similar result was obtained using (NPNA)$_{40}$ in the ELISA instead of the peptide−BSA conjugate (data not shown). This indicates that the antisera to the P^{Me}-containing peptide is able to efficiently recognize the native sequence. The two antisera were then tested for reactivity with live *P. falciparum* sporozoites by solid-phase immunofluorescent assay. Both antisera recognized the sporozoites with comparable activity in the immunofluoresence assay; each antiserum could be diluted up to 6000-fold, before the fluorescence became too weak to detect, indicating in both a high titer of anti-sporozoite

(33) Güntert, P.; Braun, W.; Billeter, M.; Wüthrich, K. *J. Am. Chem. Soc.* **1989**, *111*, 3997.
(34) Güntert, P.; Braun, W.; Wüthrich, K. *J. Mol. Biol.* **1991**, *217*, 517.
(35) van Gunsteren, W. F.; Berendsen, H. J. C. In *Biomos;* Groningen, The Netherlands, 1987.
(36) Wilmot, C. M.; Thornton, J. M. *J. Mol. Biol.* **1988**, *203*, 221.
(37) Milner-White, E. J.; Bell, L. H.; Maccallum, P. H. *J. Mol. Biol.* **1992**, *228*, 725.
(38) Mádi, Z. L.; Griesinger, C.; Ernst, R. R. *J. Am. Chem. Soc.* **1990**, *112*, 2908.

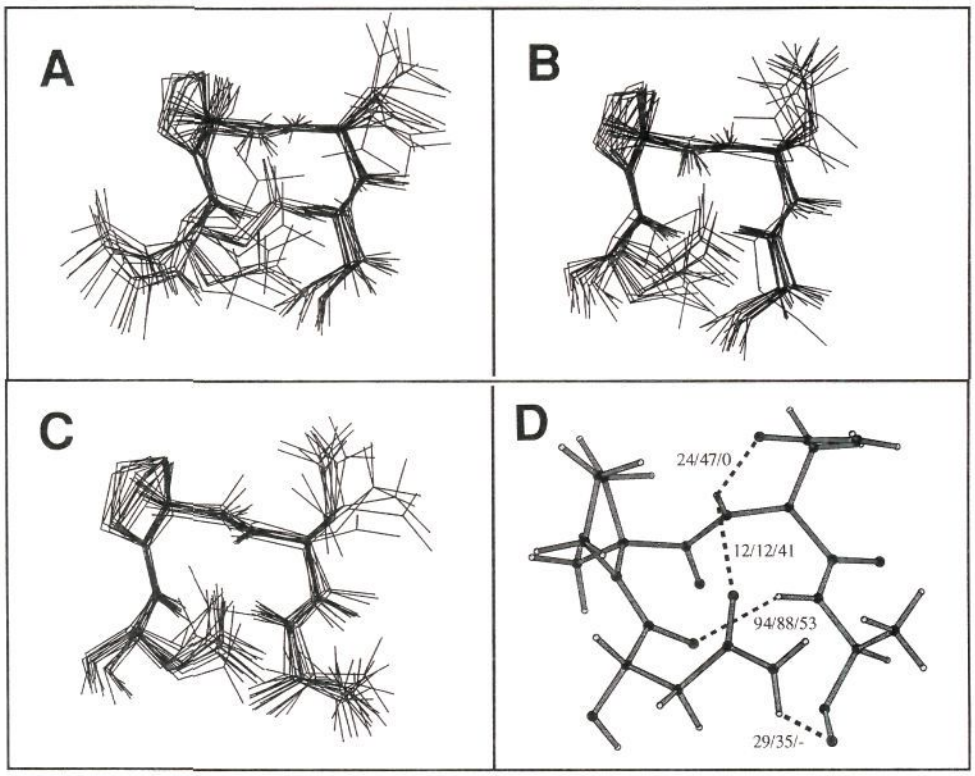

Figure 6. Superimposition of (A) the first, (B) the second, and (C) the third $NP^{Me}NA$ motifs from within the final 17 MD refined structures of the peptide Ac-$(NP^{Me}NA)_3$-OH (see text). In D the numbers give the frequency (%) with which hydrogen bonds (indicated by dashed lines) were detected in the first/second/third $NP^{Me}NA$ β-turn motifs in these 17 structures.

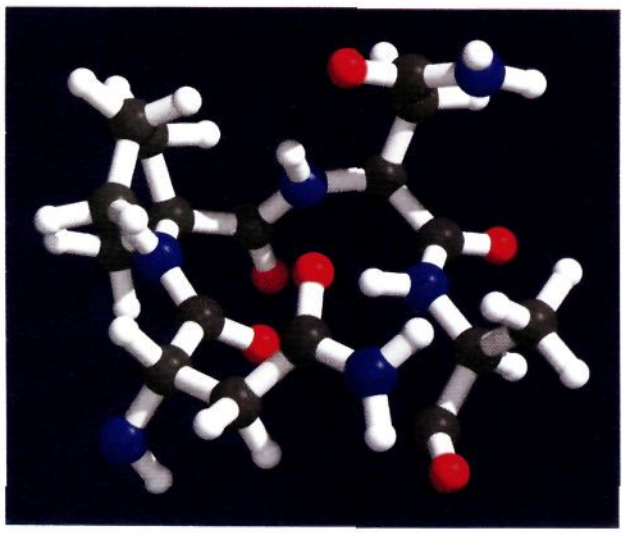

Figure 7. Color representation of one typical β-turn conformation found within the $NP^{Me}NA$ motif (compare Figure 6), prepared using the programs Molscript[64] and Raster3D.[65]

antibodies. This provides strong evidence that the P^{Me}-containing peptide adopts conformations that mimic portions of the folded, immunologically active sporozoite surface protein.

Discussion

Application of the Chou and Fasman secondary structure prediction method[39] suggests that the NPNA tetrapeptide motif has a high intrinsic probability of adopting β-turn conformations. Earlier CD and NMR studies[18] in water provided experimental support for this prediction, by showing that synthetic peptides containing the NPNA motif, either singly or in tandemly repeated copies, adopt either a single turn structure or an interlinked series of turn conformations, respectively, although not a continuous helix. The CD and NMR spectra described here show that replacing proline by (*S*)-α-methylproline (P^{Me})

(39) Chou, P. Y.; Fasman, G. D. *Adv. Enzymol.* **1978**, *47*, 45.

Table 3. Summary of Input Constraints for the Structure Calculations and the Violations, RMSDs, and Energies of the Final 17 Structures of Ac-$(NP^{Me}NA)_3$-OH[a]

Input to Structure Calculations		
$^1H-^1H$ distance constraints		
total	67	
intraresidue	24	
sequential	23	
medium range	20	
dihedral angle constraints[b]	21	
stereospecific assignments	Asn 1, Asn 5, Asn 9	
total constraints/residue	5.6	
Results of Structure Calculations		
energy (kcal mol^{-1})		
total	-946 ± 35	$-1012...-897$
nonbonded	-238 ± 16	$-261...-195$
restraint violation	15 ± 3	11...23
NOE violations		
number > 0.1 Å	7.2 ± 2.2	4...12
number > 0.2 Å	1.8 ± 1.5	0...4
maximum (Å)	0.23 ± 0.05	0.18...0.35
sum (Å)	1.52 ± 0.41	0.81...2.31
pairwise RMSD (Å)		
all backbone atoms	2.64 ± 2.34	0.33...5.44
turn 1	0.56 ± 0.27	0.09...1.27
turn 2	0.51 ± 0.22	0.09...1.03
turn 3	0.41 ± 0.23	0.08...1.08
all turns	0.65 ± 0.25	0.08...1.28

[a] Results are listed as average ± standard deviation and range of observed values (low...high), within each individual $NP^{Me}NA$ motif. [b] The angle constraints were only used in the distance geometry calculations with DIANA.

Table 4. Observed Torsion Angles, with Standard Deviation and Range, Found in the 17 MD-Refined Structures

residue	torsion	angle	std dev	range
Asn 1	ψ	108.62	±14.19	86.97...133.42
	χ^1	163.42	±45.42	39.27...−156.84
	χ^2	13.97	±40.94	−78.38...75.12
P^{Me} 2	ϕ	−20.80	±8.19	−31.92...−4.75
	ψ	−67.56	±17.44	−97.25...−44.40
Asn 3	ϕ	−80.79	±17.01	−113.09...−49.95
	ψ	−13.20	±23.45	−52.35...25.72
	χ^1	8.40	±99.81	−148.86...153.91
	χ^2	−4.70	±97.98	−132.54...152.12
Ala 4	ϕ	−126.88	±22.34	−161.44...−84.65
	ψ	56.82	±15.96	12.61...78.80
Asn 5	ϕ	−94.31	±31.83	−143.84...−34.67
	ψ	103.78	±15.04	80.44...132.06
	χ^1	−173.93	±34.67	50.51...−144.91
	χ^2	29.71	±28.95	−28.36...87.56
P^{Me} 6	ϕ	−20.08	±6.19	−30.45...−7.40
	ψ	−70.79	±13.25	−93.76...−48.47
Asn 7	ϕ	−74.93	±10.70	−99.83...−58.59
	ψ	−27.09	±15.79	54.29...11.86
	χ^1	−28.48	±49.61	−69.50...67.34
	χ^2	34.97	±69.02	−87.04...100.89
Ala 8	ϕ	−111.81	±45.48	−157.78...52.96
	ψ	62.75	±13.28	35.56...83.66
Asn 9	ϕ	−102.52	±27.50	−144.34...−19.71
	ψ	109.47	±11.53	96.99...130.57
	χ^1	−171.14	±11.56	169.82...−139.11
	χ^2	4.56	±32.66	−73.04...94.32
P^{Me} 10	ϕ	−30.04	±4.84	−39.27...−22.82
	ψ	−52.07	±10.52	−70.33...−32.15
Asn 11	ϕ	−98.63	±15.82	−120.31...−61.03
	ψ	40.56	±23.17	−11.83...66.88
	χ^1	−74.19	±61.90	−169.17...53.11
	χ^2	92.15	±68.61	−88.96...169.35
Ala 12	ϕ	−66.49	±34.50	−116.10...35.96

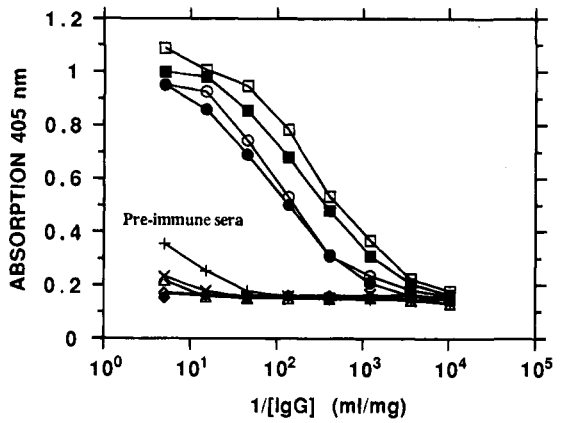

Figure 8. ELISA results for reactions of IgG fractions from rabbit antisera raised against KLH-C($NP^{Me}NA$)$_3$-OMe (A) and KLH-C(NPNA)$_3$-OMe (B) (each raised in duplicate). The data for antisera A binding to BSA-C($NP^{Me}NA$)$_3$-OMe (●) and BSA-C(NPNA)$_3$-OMe (○) and antisera B binding to BSA-C($NP^{Me}NA$)$_3$-OMe (■) and BSA-C(NPNA)$_3$-OMe (□) are given. Controls without IgG (◆) and with preimmune sera are also shown.

in this -NPNA- motif leads to the strong stabilization of β-turn conformations in aqueous solution.

It is not straightforward to deduce unambiguously from the CD spectra alone which types of turn conformation in Ac-(NP^{Me}NA)$_3$-OH are preferentially populated. An α-helical conformation is not expected since proline is strongly disfavored within a regular α-helix, except in the N-terminal first turn.[40] In considering the eight subclasses of β-turns discussed by Wilmot and Thornton,[36] only type-I and type-II turns are strongly expected for the NPNA motif. An analysis of β-turns in protein X-ray crystal structures showed that Asn has a higher than average frequency of occurrence at position *i*, and proline at position $i + 1$, of a type-I β-turn. The type-I′ and type-II′ turns are sterically more compatible with D-amino acids or glycine at the $i + 2$ position, whereas type-VI turns usually require a *cis*-Xaa-Pro peptide bond. CD spectroscopy has been used to distinguish between pure type-I and type-II turns,[41] with type-I turns correlating with spectra resembling those from α-helixes (negative peak at ≈200 nm and weak shoulder at ≈220 nm) and type-II turns showing a positive CD peak at ≈200 nm. On this basis, Ac-($NP^{Me}NA$)$_3$-OH appears to prefer type-I β-turns, a conclusion which is also supported by the NMR data. However, the possibility of distorted turn conformations, including other turn types (e.g., γ-turns), of conformational averaging, and in this case the clear indication from NMR that the side chains of both Asn residues adopt preferred conformations relative to the peptide backbone, complicate the interpretation of the CD data.

The NMR spectra, however, provide clear evidence for a highly populated type-I β-turn in each $NP^{Me}NA$ motif in the peptide Ac-($NP^{Me}NA$)$_3$-OH. In particular:

(1) the lower temperature coefficients for the chemical shifts of the Asn ($i + 2$) and, in particular, the Ala ($i + 3$) amide protons, in the peptide Ac-($NP^{Me}NA$)$_3$-OH (Table 2), indicate that these amide protons are shielded from the bulk solvent. The Ala ($i + 3$) amide proton is expected to form a hydrogen bond to the peptide carbonyl group of Asn (*i*) in a β-turn conformation.

(2) the appearance of a series of medium-range (i, $i + 3$) NOE connectivities in NOESY and ROESY spectra between the Asn (i) side chain and the Ala ($i + 3$) residue (Figures 3 and 5A), and a particularly strong d_{NN} NOE connectivity between Asn ($i + 2$) and Ala ($i + 3$) (Figure 4B), point to a high population of turn conformations within each $NP^{Me}NA$ motif. It is noteworthy that, although similar medium-range NOE cross peaks are seen in the NOESY spectra of Ac-(NPNA)$_3$-OH, their relative intensity is low, and specific NOE assignments are made difficult by spectral overlap (Figure- 5B). Thus it appears that the introduction of the α-methyl group stabilizes a pre-existing peptide backbone conformation, rather than forcing the peptide into new types of secondary structure. This conclusion is also consistent with CD spectra, where methylated and native peptide sequences have CD curves of similar shapes (Figure 2), and the similar immunological properties of the methylated and native peptides (*vide supra*).

(3) the nonaveraged $^3J_{\alpha\beta 2}$ and $^3J_{\alpha\beta 3}$ coupling constants within each Asn residue indicate that there are preferred χ_1 torsion angles for both Asn residues in each $NP^{Me}NA$ motif (Table 2). From the Karplus equation, the predicted $^3J_{\alpha\beta}$ values for a staggered conformation about the $\alpha\beta$ bond are either both ≈3.4 Hz (for $\chi_1 = 60°$) or ≈12.9 and ≈3.4 Hz (for = 180°, −60°), whereas for free rotation, both coupling constants are predicted to be ≈6.6 Hz. However, even slight fluctuations around the average χ_1 value will reduce the observed large coupling constant and increase the observed small coupling constant.[42,43]

(40) MacArthur, M. W.; Thornton, J. M. *J. Mol. Biol.* **1991**, *218*, 397.

(41) (a) Perczel, A.; Hollosi, M. P. S.; Fasman, G. D. *Int. J. Pept. Protein Res.* **1993**, *41*, 223. (b) Perczel, A.; Hollósi, M.; Foxman, B. M.; Fasman, G. D. *J. Am. Chem. Soc.* **1991**, *113*, 9772. (c) Gierasch, L. M.; Deber, C. M.; Madison, V.; Niu, C.-H.; Blout, E. R. *Biochemistry* **1981**, *20*, 4730. (d) Bandekar, J.; Evans, D. J.; Krimm, S.; Leach, S. J.; Lee, S.; McQuie, J. R.; Minsian, E.; Némethy, G.; Pottle, M. S.; Scheraga, H. A.; Stimson, E. R.; Woody, R. W. *Int. J. Pept. Protein Res.* **1982**, *19*, 187. (e) Woody, R. In *Peptides, Polypeptides and Proteins*; Blout, E. R., Bovey, F. A., Lotan, N., Goodman, M., Eds.; J. Wiley: New York, 1985; pp 338−360.

(42) Hoch, J. C.; Dobson, C. M.; Karplus, M. *Biochemistry* **1985**, *24*, 3831.

For each Asn (i) residue a strong $d_{\alpha\beta}$ NOE connectivity to only one β-proton and not to the other, and medium strength $d_{N\beta}$ connectivities of equal magitude to both CβH's, are observed. On the other hand, for each Asn ($i + 2$) residue, strong $d_{\alpha\beta}$ connectivities to both β-protons, but only one strong $d_{N\beta}$ connectivity, are seen. On the basis of these coupling and NOE data it was possible using the program HABAS[33] to derive an unambiguous stereospecific assignment for the Asn (i) β-protons, but not for the Asn ($i + 2$) β-H's.

The results described above provide mutually supportive and interlocking evidence that a family of closely related turn conformations are highly populated in each NP^{Me}NA motif. *Although it must be assumed that these turns are in dynamic equilibrium with unfolded forms*, they most likely occur in greater than 50% of the population at any one time. An accurate estimate of the population frequency is at present difficult to derive, but an approach used previously[44] for such a purpose makes use of the amide proton temperature coefficient of the ($i + 3$) residue in the turn to estimate the population of intramolecular backbone-to-backbone hydrogen-bonded forms. We assume that the highest attainable temperature coefficient for the Ala amide proton in each turn, corresponding to an unfolded structure, lies in the range -7 to -9 ppb/K, and the lowest value, corresponding to complete Asn (i) CO to Ala ($i + 3$) NH hydrogen bond and hence turn formation, is close to 0 ppb/K. A linear correlation between the population of the β-turn and the temperature coefficient leads to estimates of $\approx$ 70%, 80%, and 80% β-turn formation in the first, second, and third NP^{Me}NA motifs, respectively (Table 2). On the other hand, similar arguments applied to the NPNA motifs suggest a fractional turn population of about 10$-$20%, based on the temperature coefficients for the Ala NH resonances.

Given a high turn population in the conformational ensemble, it becomes interesting to perform structure calculations based upon distance and dihedral angle constraints derived from the NMR data. Indeed, only if the structured forms exist at high frequency are the resulting structures likely to resemble conformers actually present in the ensemble in solution.[45] In this case, distance geometry and restrained molecular dynamics calculations indicate that a type-I β-turn conformation is preferentially stabilized in each NP^{Me}NA motif. It should be emphasized that a very conservative NOE to distance conversion has been used in this study, which does provide some allowance for contributions from unfolded forms. Indeed, the presence of other conformers in the ensemble is indicated by the $d_{\alpha N}$ (i, $i + 1$) NOEs between the P^{Me} and the following Asn, which are incompatible with a type-I turn. These are also present at higher intensities, in the native peptide where the turns are less highly populated. Nevertheless, the structure calculations, which were performed on the full NOE data set to avoid biasing their outcome toward a preconceived conformation, converge to a single family of backbone conformers within each motif, which are both energetically plausible and consistent with all the experimental data. The good convergence is achieved, despite conservative constraints, due to the large number of medium-range NOEs observed across each turn motif. These results strongly indicate that the type-I β-turn conformation is present in the majority of backbone conformers present in solution. The calculations also show which ranges of χ_1 angles are likely for the Asn side chains (see Figure 6, Table 4). The side chain of each Asn (i) residue is quite well defined in all 17 structures, with a χ_1 angle close to 180°, which allows the side chain amide carbonyl group to hydrogen bond to the Asn ($i + 2$) peptide NH group (see also Figure 7). This mirrors a well-known tendency for the side chain of Asn at position i of type-I β-turns in protein crystal structures to hydrogen bond with the backbone peptide NH group of residue $i + 2$.[36] This side chain$-$backbone hydrogen bond, in addition to the expected i to $i + 3$ backbone$-$backbone hydrogen bond and the α-methyl group, could impart significant stabilization to the type-I β-turn conformation. Asparagine is also quite common at position $i + 2$ of type-I β-turns.[36] In the structures calculated here, a wider variation in χ_1 angles for each Asn ($i + 2$) residue is apparent (Figure 6 and Table 4). This results from relaxed local constraints which arise due to the lack of stereospecific assignments for the CβH's of these residues. It is interesting to note, however, that there is again a tendency for side chain$-$backbone hydrogen bonding involving the Asn ($i + 2$) backbone NH group (Figures 6 and 7).

No regular, repeating conformations were detected in the linker regions connecting individual NP^{Me}NA motifs. Therefore, although the motif itself appears well defined, it is not clear how they might be joined to produce a global polypeptide fold. Computer modeling studies by Brooks and co-workers,[46] and by Scheraga and co-workers,[47,48] explored a large number of helical or near-helical conformations for a tandemly repeated NPNA peptide. In the former study,[46] the best helical structure calculated was a right-handed 12_{38} helix with a pitch of 4.95 Å and a diameter of $\approx$17 Å. This is unlike the structures derived in our work, since the NPNA motifs in this 12_{38} helix contain a distorted type-II β-turn and a quite different pattern of hydrogen bonds. Gibson and Scheraga,[47] on the other hand, found two low-energy helical conformations for tandemly repeated NPNA peptides, but for the same reasons, these appear from the published stereodiagrams to be unlike the conformations deduced here. However, does this mean that the type-I turns detected in this work are present in the CS protein? It is possible, for example, that a much larger tandemly repeated NPNA peptide might fold in a way which disrupts secondary structure present in smaller peptides. Our immunological results, however, do not support this view.

Small synthetic peptides containing tandemly repeated NPNA units are known to elicit a strong immune response and a high titer of anti-sporozoite antibodies,[15] as shown again in the present study. This immunological potency is believed to be a consequence of the conformational similarity of the peptides to the longer repeated sequence in the CS protein itself. The fact that an antiserum against -(NP^{Me}NA)$_3$- recognizes intact sporozoites as efficiently as an antiserum against -(NPNA)$_3$- strengthens the conclusion that the secondary structure present in this peptide is relevant, i.e. is closely related to at least portions of the folded CS protein. This result contributes to knowledge of the three-dimensional structure of the CS protein, which in turn may facilitate the design of more effective malaria vaccines. The data presented here also show that anti-sporozoite antibodies can be induced by (NP^{Me}NA)$_3$. More detailed immunological studies will be necessary, however, to explore how the antigenicity (recognition of antigen) and immunogenicity (induction of an immune response) of the peptide have been influenced by this use of methylproline. In the longer term, it will also be valuable to define and mimic the structure of neutralizing epitopes on the surface of the CS protein.

(43) Nagayama, K.; Wüthrich, K. *Eur. J. Biochem.* **1981**, *115*, 653.
(44) Dyson, H. J.; Rance, M.; Houghten, R. A.; Lerner, R. A.; Wright, P. E. *J. Mol. Biol.* **1988**, *201*, 161.
(45) Yao, J.; Dyson, H. J.; Wright, P. E. *J. Mol. Biol.* **1994**, *243*, 754.
(46) Brooks, B. R.; Pastor, R. W.; Carson, F. W. *Proc. Natl. Acad. Sci. U.S.A.* **1987**, *84*, 4470.
(47) Gibson, K. D.; Scheraga, H. A. *Proc. Natl. Acad. Sci. U.S.A.* **1986**, *83*, 5649.
(48) Roterman, I. K.; Gibson, K. D.; Scheraga, H. A. *J. Biomol. Struct. Dyn.* **1989**, *7*, 391.

Experimental Section

Peptide Synthesis General. Bromotris(pyrrolidino)phosphonium hexafluorophosphate (PyBroP), *O*-(benzotriazol-1-yl)-*N*,*N*,*N*′,*N*′-tetramethyluronium hexafluorophosphate (HBTU), 4-(*N*,*N*-dimethylamino)pyridine (DMAP), 1-hydroxy-7-azabenzotriazole (HOAt), *O*-(7-azabenzotriazol-1-yl)-*N*,*N*,*N*′,*N*′-tetramethyluronium hexafluorophosphate (HATU), *O*-(1,2-dihydro-2-oxo-1-pyridyl)-*N*,*N*,*N*′,*N*′-tetramethyluronium tetrafluoroborate (TPTU), and 1-hydroxybenzotriazole (HOBt) were analytical grade. *N*,*N*-Dimethylformamide (DMF) and 1-methyl-2-pyrrolidone (NMP) were dried over $MgSO_4$ and redistilled from ninhydrin, and *N*,*N*-diisopropylethylamine (DIEA) was redistilled from ninhydrin and KOH, just prior to use. High-performance liquid chromatography (HPLC) was carried out using a dual pump Pharmacia system and Waters RCM-μBondapak-C_{18} cartridges (10 μm, 125 Å, 25 × 100 mm) for preparative and (8 × 10 mm) analytical separations, with flow rates of 8 and 2 mL/min, respectively. UV detection was at 226 and 278 nm.

H-Asn-Ala-O*t*Bu. Fmoc-Asn-OH (1.77 g, 5 mmol), H-Ala-O*t*Bu·HCl (0.91 g, 5 mmol), and DIEA (1.71 mL, 10 mmol) in DMF (24 mL) were treated with HBTU (1.90 g, 5 mmol) in portions and stirred for 2.5 h at room temperature. The reaction mixture was then diluted with EtOAc (600 mL), washed with 0.05 N HCl (2 × 250 mL), saturated $NaHCO_3$ (2 × 250 mL), and saturated brine. The organic phase was dried (Na_2SO_4) and concentrated *in vacuo*. The resulting solid was then stirred with 20% piperidine in DMF for 2 h. The reaction mixture was concentrated *in vacuo* and triturated with diethyl ether. Recrystallization from EtOAc gave the product as a colorless solid (1.02 g, 3.93 mmol, 79%): mp 117−118 °C; $[\alpha]^{21}_D = -26.8°$ (c = 1.0, DMF); ^{1}H-NMR (300 MHz, DMSO-d_6) δ 8.13 (d, J = 7.1, 1H), 7.37 (br. s, 1H), 6.82 (br. s, 1H), 4.11 (dq, J = 7.3, 7.1, 1H), 3.48 (dd, J = 9.4, 3.6, 1H), 2.39 (dd, J = 15.0, 3.6, 1H), 2.14 (dd, J = 15.0, 9.5, 1H), 1.39 (s, 9H), 1.24 (d, J = 7.3, 3H); CI-MS 260.1 (M + H, 100), 204.0 (M − 55, 36).

H-P^{Me}-Asn-Ala-O*t*Bu. Dipeptide H-Asn-Ala-O*t*Bu (660 mg, 2.55 mmol), Fmoc-P^{Me}-OH[19] (813 mg, 2.31 mmol), and DIEA (396 μL, 2.31 mmol) in DMF (8 mL) were treated with HBTU (1.05 g, 2.78 mmol). After being stirred for 2 h at room temperature the reaction mixture was diluted with dichloromethane and washed with 0.05 N HCl and saturated $NaHCO_3$. After drying ($MgSO_4$) and concentration *in vacuo*, the resulting solid was treated with 20% piperidine in DMF. The reaction mixture was concentrated *in vacuo* and triturated with diethyl ether to give the product as a colorless solid from EtOAc (0.8 g, 85%): mp 166−168 °C; $[\alpha]^{21}_D = -30.5°$ (c = 1.0, DMF); ^{1}H NMR (300 MHz, DMSO-d_6) δ 8.39 (d, J = 8.6, 1H), 8.10 (d, J = 7.0, 1H), 7.30 (br. s, 1H), 6.90 (br. s, 1H), 4.45−4.51 (m, 1H), 4.08 (dq, J = 7.1, 7.0, 1H), 2.91−2.97 (m, 1H), 2.65−2.71 (m, 1H), 2.38−2.49 (m, 2H), 1.96- 2.03 (m, 1H), 1.39−1.63 (m, 3H), 1.37 (s, 9H), 1.22 (s, 3H), 1.22 (d, J = 7.1, 3H); CI-MS 371.3 (M + H, 100).

Fmoc-NP^{Me}NA-OH, H-N(Tmb)P^{Me}NA-O*t*Bu, and Ac-NP^{Me}NA-OH. Tripeptide H-P^{Me}-Asn-Ala-O*t*Bu (600 mg, 1.62 mmol), Fmoc-Asn(Tmb)-OH (1.06 g, 1.98 mmol), and DIEA (610 μL, 3.56 mmol) were treated with PyBroP (924 mg, 1.98 mmol) at 4 °C. After being stirred for 23 h at 4 °C the reaction mixture was diluted with EtOAc and washed with 5% NaH_2PO_4, followed by saturated $NaHCO_3$ and brine. After drying ($MgSO_4$), the product was purified by silica flash chomatography (6% MeOH/EtOAc, R_f = 0.18) to give Fmoc-N(Tmb)P^{Me}NA-O*t*Bu (1.24 g, 86%). A portion of this (400 mg, 0.45 mmol) was treated with 5% ethanedithiol in TFA and then concentrated *in vacuo* and triturated with diethyl ether to afford Fmoc-NP^{Me}NA-OH (269 mg, 92%): ES-MS 651.3 (M + H), 673.2 (M + Na). Anal. Calcd for $C_{32}H_{38}N_6O_9$: C, 59.1; H, 5.9; N, 12.9. Found: C, 59.1; H, 5.6; N, 12.8. A further portion of Fmoc-N(Tmb)P^{Me}NA-O*t*Bu (60 mg, 0.068 mmol) was dissolved in 20% piperidine/DMF, concentrated *in vacuo*, and triturated with diethyl ether to afford H-N(Tmb)P^{Me}NA-O*t*Bu (66 mg, 88%): ES-MS 665.6 (M + H), 687.5 (M + Na). This was acetylated by treatment with 5% Ac_2O in DMF. Concentration *in vacuo*, trituration with diethyl ether, and purification by HPLC (linear gradient 25−80% acetonitrile in water + 0.1% TFA over 30 min) gave Ac-N(Tmb)P^{Me}NA-O*t*Bu, which was then treated with 5% ethanedithiol in TFA for 2 h. Concentration *in vacuo*, trituration with diethyl ether, and purification by HPLC (0−25% acetonitrile in water + 0.1% TFA) gave Ac-NP^{Me}NA-OH (23 mg): ES-MS 471.0 (M + H), 493.7 (M + Na); ^{1}H NMR see text.

Solution-Phase Synthesis of Ac-(NP^{Me}NA)$_2$-OH and Ac-(NP^{Me}NA)$_3$-OH. Fmoc-NP^{Me}NA-OH (30 mg, 0.046 mmol) and H-N(Tmb)P^{Me}NA-O*t*Bu (30 mg, 0.045 mmol) were mixed with HOBt (14 mg, 0.091 mmol) and DIEA (17 μL, 0.099 mmol) in DMF (1.5 mL) at 0 °C. TPTU (17 mg, 0.057 mmol) was added with stirring at 4 °C for 14 h. EtOAc was then added (60 mL), and the solution was washed with 5% NaH_2PO_4 and then saturated $NaHCO_3$. After drying ($MgSO_4$) and concentration *in vacuo*, Fmoc-NP^{Me}NAN(Tmb)P^{Me}NA-O*t*Bu was obtained: ES-MS 1297.8 (M + H), 1319.7 (M + Na). This was treated sequentially with 20% piperidine in DMF, acetic anhydride, and then 5% ethanedithiol in TFA, to afford Ac-(NP^{Me}NA)$_2$-OH; ES-MS 881.7 (M + H), 903.6 (M + Na); ^{1}H NMR see text. H-NP^{Me}-NAN(Tmb)P^{Me}NA-O*t*Bu (32 mg) was reacted with Fmoc-NP^{Me}NA-OH using the same conditions as above. The product was purified by preparative HPLC (linear gradient of 30 to 95% MeOH in water + 0.1% TFA over 35 min) to give Fmoc-(NP^{Me}NA)$_2$N(Tmb)P^{Me}NA-O*t*Bu (48 mg, 94%): ES-MS 854.7 (M + 2H), 1730.0 (M + Na). This was treated sequentially with 20% piperidine in DMF and 5% acetic anhydride in DMF. Purification by HPLC gave Ac-(NP^{Me}NA)$_2$N(Tmb)-P^{Me}NA-O*t*Bu (41 mg, 95%); ES-MS 1550.2 (M + Na). Treatment with 5% ethanedithiol in TFA followed by concentration *in vacuo*, trituration with diethyl ether, and HPLC purification (linear gradient of 0 to 20% acetonitrile in water + 0.1% TFA over 20 min) gave Ac-(NP^{Me}NA)$_3$-OH (31 mg, 89%); ES-MS 1313.8 (M + Na), 668.6 (M + 2Na); ^{1}H NMR see text.

Fmoc-C(Acm)NP^{Me}NA-OH. H-N(Tmb)P^{Me}NA-O*t*Bu (50 mg, 0.075 mmol), Fmoc-Cys(Acm)-OH (35 mg, 0.084 mmol), HOBt (15 mg, 0.1 mmol), and DIEA (30 μL, 0.175 mmol) in DMF (2 mL) were treated with HBTU (39 mg, 0.103 mmol) at 0 °C, and the reaction mixture was left at 4 °C overnight. After dilution with EtOAc, washing with 5% NaH_2PO_4 and then saturated $NaHCO_3$, drying ($MgSO_4$), and concentration *in vacuo*, the product was treated with 5% ethanedithiol in TFA, again concentrated *in vacuo*, and triturated with ether to give product (57 mg, 92%): ES-MS 825.2 (M + H), 847.7 (M + Na).

Ac-C(NP^{Me}NA)$_3$-OMe. H-NP^{Me}NAN(Tmb)P^{Me}NA-O*t*Bu (73 mg, 0.068 mmol), Fmoc-C(Acm)NP^{Me}NA-OH (55 mg, 0.068 mmol), HOBT (18 mg, 0.118 mmol), and DIEA (33 μL, 0.193 mmol) in DMF (2.5 mL) were treated with TPTU (25 mg, 0.084 mmol) at 0 °C. After being stirred overnight at 4 °C and concentration *in vacuo*, purification by HPLC (linear gradient of 30 to 95% MeOH in water + 0.1% TFA over 35 min) gave the product (106 mg, 82%). Subsequent treatment with 5% ethanedithiol in TFA, concentration *in vacuo*, and purification by HPLC, as above, gave the free acid (80 mg, 86%): ES-MS 845.8 (M + 2Na), 1668.3 (M + Na). This was dissolved in MeOH and treated with a solution of diazomethane in ether. Concentration *in vacuo*, followed by treatment with 20% piperidine in DMF, concentration again *in vacuo*, acetylation with 5% acetic anhydride in DMF, and subsequent purification by HPLC (linear gradient of 0 to 20% acetonitrile in water + 0.1% TFA over 22 min) gave Ac-C(Acm)-(NP^{Me}NA)$_3$-OMe (39 mg, 54%): ES-MS 1502.1 (M + Na). A portion of this peptide (9 mg, 0.006 mmol) and $Hg(OAc)_2$ (5.8 mg, 0.018 mmol) was dissolved in water and stirred under N_2. The pH was adjusted to 4 and kept constant for 4.5 h. After the addition of dithiothreitol (10.3 mg, 0.067 mmol), the suspension was clarified by centrifugation and the product was purified by HPLC (as above) to give product (4.7 mg, 55%): ES-MS 1417.2 (M + Na).

Ac-C(NPNA)$_3$-OMe. This peptide was synthesized on an ABI 430A peptide synthesizer, using Fastmoc chemistry with a 4-fold exess of amino acid (Fmoc-Asn(Mtt)-OH, Fmoc-Ala-OH, Fmoc-Cys(Acm)-OH, and Fmoc-Pro-OH) for each 30 min coupling step. The synthesis was performed on 0.25 mmol of *p*-alkoxybenzyl alcohol resin (0.97 mmol/g). By following a standard protocol, the first Fmoc-protected amino acid was coupled twice to the resin with DCC/HOBt activation in NMP with DMAP catalysis. Subsequent coupling steps were performed with HBTU/HOBT/DIEA activation in NMP. Piperidine 20% in NMP was used to remove the Fmoc groups. After N-acetylation of the fully assembled peptide, portions of the resin were treated with 5% ethanedithiol and 4% triisopropylsilane in TFA. After filtration and purification by HPLC (linear gradient of 4 to 25% acetonitrile in water + 0.1% TFA over 18 min) Ac-C(Acm)-(NPNA)$_3$-OH was obtained in

55% yield: ES-MS 1446.1 (M + Na). The peptide in methanol was then treated with diazomethane in diethyl ether to afford Ac-C(Acm)-(NPNA)$_3$-OMe: ES-MS 719.9 (M+2H). The Acm-protecting group was removed using $Hg(OAc)_2$ as described above to afford Ac-C(NPNA)$_3$-OMe: ES-MS 706.0 (M + 2Na), 1367.8 (M + H), 1390.4 (M + Na).

Ac-(NPNA)$_3$-OH. This was obtained using the same procedure as above, except the last coupling step with Fmoc-Cys(Acm)-OH was omitted: ES-MS 1272.7 (M + Na), 647.4 (M + 2Na); ^{1}H-NMR (600 MHz, 10% D_2O/H_2O, pH 5) δ 8.37 (d, J = 7.2, 2H), 8.36 (d, J = 6.3, 1H), 8.34 (d, J = 6.6, 1H), 8.33 (d, J = 7.8, 2H), 7.97 (d, J = 6.2, 1H), 7.95 (d, J = 6.0, 1H), 7.66 (d, J = 6.8, 1H), 7.66 (s, 3H), 7.63 (s, 1H), 7.62 (s, 2H), 7.00 (s, 1H), 6.99 (s, 1H), 6.98 (s, 1H), 6.94 (s, 2H), 6.93 (s, 1H), 4.94−4.99 (m, 3H), 4.44 (dd, J = 8.3, 4.1, 1H), 4.43 (dd, J = 8.2, 4.6, 1H), 4.42 (dd, J = 8.4, 4.1, 1H), 4.24−4.30 (m, 2H), 4.11 (dq, J = 7.2, 6.8, 1H), 3.82−3.88 (m, 1H), 3.75−3.82 (m, 5H), 2.83−2.90 (m, 6H), 2.68−2.74 (m, 6H), 2.26−2.34 (m, 3H), 1.93−2.07 (m, 9H), 2.00 (s, 3H), 1.38 (d, J = 7.2, 6H), 1.35 (d, J = 7.2, 3H).

Solid-Phase Synthesis of Ac-(NP^{Me}NA)$_3$-OH. This synthesis was carried out on Fmoc-Ala-KA resin (1.05 g, 0.1 mmol/g, Novabiochem) using a Biolynx 4175 semiautomatic peptide synthesizer (Pharmacia). Peptide couplings were performed with 3 equiv of each Fmoc-protected amino acid, HBTU/HOBt and DIEA, for 2 h. Couplings onto P^{Me} residues were performed using 3 equiv of HATU/HOAt instead of HBTU/HOBt. Kaiser tests[49] indicated incomplete coupling of Fmoc-Asn(Mtt)-OH onto Ala-8, P^{Me}-6, and P^{Me}-2, even after four coupling cycles of 2 h each, so capping was performed with benzoic anhydride. The fully assembled peptide was acetylated with 5% acetic anhydride in DMF. A portion of the resin was treated with 5% ethanedithiol and 4% triisopropylsilane in TFA for 2 h at room temperature. After filtration and washing with TFA, the filtrate was concentrated *in vacuo* and the product was precipitated with diethyl ether and purified by HPLC (linear gradient from 0 to 20% acetonitrile in water + 0.1% TFA over 20 min). Ac-(NP^{Me}NA)$_3$-OH was obtained in 26% yield.

CD Spectroscopy. CD spectra were measured on a Jasco J-500A spectrometer using a cell of 1 mm path length. The average of three scans over the range 190−260 nm are given. Peptide concentrations, determined by quantitative amino acid analysis, were 210 μM for Ac-(NPNA)$_3$-OH and 310 μM for Ac-(NP^{Me}NA)$_3$-OH.

NMR Spectroscopy. All experiments were performed in water (90% H_2O/10% D_2O, pH 5.0). NMR spectra were recorded on Bruker AM300 and AMX600 spectrometers at ≈15 mM peptide concentration. 2D data sets were measured at 278 and 300 K at 600 MHz, with presaturation during the recycle delay to suppress the water resonance. Quadrature detection employed the TPPI[50] or TPPI-States[51] methods. Proton DQF-COSY,[52] TOCSY[53,54] (mixing time, t_m = 100 ms), ROESY[55] (t_m = 100, 200, and 300 ms), and NOESY[56,57] (t_m = 100, 200 and 300 ms) spectra were acquired with 1024 complex points over a spectral width of typically 6667 Hz with 512 real (TPPI) or 256 complex points in t_1. A cosine window was used for apodization in both dimensions and the data zero-filled to yield matrixes of 1024 × 2048 real points. Data processing was performed with the software FELIX v2.30 (Biosym, Inc.).

The NOESYspectra were peak picked using the tools available in FELIX. The cross peak volumes were optimized for overlapping peaks by fitting two-dimensional Gaussian functions to the total intensity in a given region. Distances were then estimated by setting the $d_{\alpha N}$ distance between Ala 4 and Asn 5 as well as Ala 8 and Asn 9 to 2.2 Å and calculating other distances according to the r^{-6} relationship, using three models: (1) assuming a linear NOE buildup to 200 ms mixing time and using the cross peak volumes at 200 ms to determine distances; (2) fitting a straight line to the build-up curve, from which distances were then extracted; (3) fitting the function $v = a_c e^{a_1 x}$ to the build-up curve and then extracting distances (r) from the linear term. A distance that was >0.3 Å longer when calculated by method 3 in comparison to that obtained from method 2 reliably indicated spin diffusion, as could be cross-checked by visual inspection of the build-up curve, and these distances were set to 5 Å. From ROESY spectra with t_m = 300 ms, it was apparent that one of the two $d_{N\beta}$ cross peaks in Asn (i + 2) arose largely due to spin diffusion. This distance was therefore assigned a lower limit of 3.0 Å. It was found that distances between 2.2 and 4.0 Å could be reliably quantified by the combined use of these methods. Torsion angle constraints for structure calculations were obtained with the software HABAS[33] (see the Results).

Structure Calculation. Structures were calculated on the basis of upper and lower distance constraints, as well as torsion angle constraints (Table 3), using the software DIANA.[34] The weighting factor for steric constraints was 0.2 up to the last level of calculation, where this factor was incremented over several steps to 2.0. All other weighting factors were used at their default values. To improve convergence, a hydrogen bond constraint between the Asn (i) CO and Ala (i + 3) NH was included by constraining the NH−O and N−O distances to 2.0 ± 0.2 and 3.0 ± 0.2 Å, respectively, because preliminary calculations had indicated that this bond was formed in most converged structures. The peptide amide temperature coefficient of Ala (i + 3) residues also indicate the presence of a hydrogen bond (Table 2). This hydrogen bond constraint was removed at the final level of the DIANA calculation, and the structures were minimized against the experimental data only. The first 25 structures with a final target function value below 0.1 Å^2 were accepted for restrained molecular dynamics (MD) refinement, using the program GROMOS and the 37D4 force field.[35]

Each of the starting conformations was refined to the upper bound constraints between atoms i and j (r_{ij}^{ub}) according to the following equation:[58]

$$V_{restr}^{dr} = {}^1/_2 k^{dr} \sum_{\text{NOE pairs } (i,j)} [\text{MAX}(0, r_{ij} - r_{ij}^{ub})]^2$$

so that the total potential energy

$$V_{total} = V_{physical} + V_{restr}^{dr}$$

attains a reasonable minimum. In the MD calculations the covalent bond lengths were constrained using the SHAKE procedure[59] with relative tolerance of 10^{-4}. The time step used in the leap-frog integration scheme was δ_t = 0.002 ps. A cutoff radius of 8.5 Å for the nonbonded interactions was used in conjunction with a pair list that was updated every 10 time steps. The MD was performed at 300 K by coupling the system to a heat bath.[60] Details of the atom−atom treatment of the distance restraining are described by van Gunsteren et al.[61] For each of the 25 starting structures 50 steps of energy minization were performed with a force constant k^{dr} = 500 kJ/(mol·Å^2) to the distance restraints, to remove initial close contacts. Then 10 ps of MD was performed using a force constant k^{dr} = 5000 kJ/(mol·Å^2). Each structure was further minimized to convergence with the higher force constant. The energy of each of these structures went from an intial value of 10^6 to -10^3 kJ/mol. Conformations of the peptide were eliminated if any of the remaining distance constraint violations were greater than 0.35 Å.

(49) Kaiser, E. T.; Bossinger, C. D.; Colescott, R. L.; Olsen, D. B. *Anal. Biochem.* **1980**, *118*, 149.
(50) Marion, D.; Wüthrich, K. *Biochem. Biophys. Res. Commun.* **1983**, *113*, 967.
(51) Marion, D.; Ikura, M.; Tschudin, R.; Bax, A. *J. Magn. Reson.* **1989**, *85*, 393.
(52) Rance, M.; Sorensen, O. W.; Bodenhausen, G.; Wagner, G.; Ernst, R. R.; Wüthrich, K. *Biochem. Biophys. Res. Commun.* **1983**, *117*, 479.
(53) Bax, A.; Davis, D. *J. Magn. Reson.* **1985**, *65*, 355.
(54) Braunschweiler, L.; Ernst, R. R. *J. Magn. Reson.* **1983**, *53*, 521.
(55) Bothner-By, A. A.; Stephens, R. L.; Lee, J.-M.; Warren, C. D.; Jeanloz, R. W. *J. Am. Chem. Soc.* **1984**, *106*, 811.
(56) Jeener, J.; Meier, B. H.; Bachmann, P.; Ernst, R. R. *J. Chem. Phys.* **1979**, *71*, 4546.
(57) Kumar, A.; Ernst, R. R.; Wüthrich, K. *Biochem. Biophys. Res. Commun.* **1980**, *95*, 1.
(58) Schiffer, C. A.; Huber, R.; Wüthrich, K.; van Gunsteren, W. F. *J. Mol. Biol.* **1994**, *241*, 588.
(59) Ryckaert, J.-P.; Ciccotti, G.; Berendsen, H. J. C. *J. Comput. Phys.* **1977**, *23*, 327.
(60) Berendsen, H. J. C.; Postma, J. P. M.; van Gunsteren, W. F.; DiNola, A.; Haak, J. R. *J. Chem. Phys.* **1984**, *81*, 3684.
(61) van Gunsteren, W. F.; Boelens, R.; Kaptein, R.; Scheek, R. M.; Zuiderweg, W. R. P. In *Molecular Dynamics and Protein Structure*; Hermans, J., Ed.; Polycrystal Bookservice: Western Springs, IL, 1985; pp 92−99.

Biochemical Assays. The peptides Ac-C($NP^{Me}NA$)$_3$-OMe and Ac-C(NPNA)$_3$-OMe were conjugated to KLH and to BSA using (*m*-maleimidobenzoyl)-*N*-hydroxysuccinimide ester.[62] Quantitative amino acid analysis indicated loadings of about ≈20−30 peptides per 10^5 Da of KLH. Two rabbits were immunized subcutaneously with each peptide−KLH conjugate (≈100 μg) in Hunter's TitreMax adjuvant, and the immunization was repeated on days 30 and 52. Ten days later the antiserums were prepared and the IgG fraction from each was isolated by protein-A affinity chromatography.[62] The secondary antibody was goat anti-rabbit IgG−alkaline phosphatase conjugate (Sigma), with *p*-nitrophenyl phosphate as the substrate. Absorbance was monitored at 405 nm.

Immunofluorescence assays were performed as described elsewhere[15b] using 12-well multitest slides coated with ≈2000 sporozoites per well. Sporozoites were from salivary glands of *Anopheles stephensii* infected with *P. falciparum* strain NF54.[63] The sera were serially diluted in PBS containing 2% BSA, and 15 μL were added to each well. After incubation at 37 °C for 15 min, the wells were washed twice with PBS/2%BSA. Goat anti-rabbit IgG conjugated to fluorescein was then added. After incubation at 37 °C for 15 min, each well was washed with PBS and water. Thereafter the slides mounted in 50% glycerol/water were analyzed under the microscope with UV illumination.

Acknowledgment. This work was supported by grants from the Swiss National Science Foundation. We are particularly grateful to Dr. H. Matile (Hoffmann-La Roche, Pharma Division, Basel, Switzerland) for providing *P. falciparum* sporozoites and $(NPNA)_{40}$ and for help with the immunofluorescence assays.

Supporting Information Available: Tables giving the distance and angle constraints used for the structure calculations (3 pages). This material is contained in many libraries on microfiche, immediately follows this article in the microfilm version of the journal, can be ordered from the ACS, and can be downloaded from the Internet; see any current masthead page for ordering information and Internet access instructions.

JA950943+

(62) Harlow, E.; Lane, D. *Antibodies: A laboratory manual*; Cold Spring Harbor Laboratory: Cold Spring Harbor, NY, 1988.
(63) Ponnudurai, T.; Lensen, A. H. W.; Leeuwenberg, A. D. E. M.; Meuwissen, J. H. E. T. *Trans. R. Soc. Trop. Med. Hyg.* **1982**, *76*, 812.
(64) Kraulis, P. J. *J. Appl. Crystallogr.* **1991**, *24*, 946.
(65) Merritt, E. A.; Murphy, M. E. P. *Acta Crystallogr.* **1994**, *D50*, 869.